

Response to comments of Reviewers

Interactive comment on “Hybrid improved EMD-BPNN model for the prediction of sea surface temperature” by Zhiyuan Wu et al.

Huang (Referee)

huanglimin@hrbeu.edu.cn

Received and published: 28 January 2019

Dr. Huang knows the topic very well and his/her comments are indeed helpful in improving the quality of this MS. We are grateful to Dr. Huang for a careful checking and comments on the MS. All comments are addressed point by point, each starting with an original comment and followed by a response in italic, as follows.

This paper proposed a hybrid EMD-BPNN model for SST prediction. The research work is very interesting and important. However, in my opinion, the paper needs minor revision before acceptance. You can find my questions and suggestions bellow.

Response: *Thank you for these comments. The positive comments in our solid professional skills are good encouragement to us.*

1. Why the simple EMD algorithm is not compared to the EEMD and CEEMD? I suggest the authors to provide comparison results of the EMD-BPNN.

Response: *Thank you for the professional comment. Empirical Mode Decomposition (EMD) is a state-of-the-art signal processing method proposed by Huang et al. This method can decompose the signal data of different frequencies step by step according to the characteristics of the data and obtain several periodic and trending signals orthogonal to each other, the method can decompose the stronger nonlinear and non-stationary signals into weaker nonlinear and non-stationary signals. The variation of SST is a deterministic non-linear dynamic system and a non-stationary time series data with intermittent signals. Once the intermittent signal is present in the actual signal, the frequency aliasing phenomenon occurs in the decomposition method of EMD, also called Mode Mixing Problem. The specific manifestation of this problem is that there are multiple scale components in one IMF component, or one scale component exists in multiple IMF components. Therefore, we carry out this research based on EEMD and CEEMD methods.*

2. Mode mixing is the motivation that the authors applied the EEMD technique in the hybrid SST prediction model. Therefore, it is very important to demonstrate the mode mixing problem in decomposing the studied SST time series. But this is not given in this paper. I suggest the authors to provide discussions on the mode mixing problem in the present study.

Response: *Thank you for your suggestion, and it is indeed a very important issue. We added the following statement to the revised manuscript.*

The variation of SST is a deterministic non-linear dynamic system and a non-stationary time series data with intermittent signals. Empirical Mode Decomposition (EMD) method can

decompose the signal data of different frequencies step by step according to the characteristics of the data and obtain several periodic and trending signals orthogonal to each other, the method can decompose the stronger nonlinear and non-stationary signals into weaker nonlinear and non-stationary signals.

However, we know that once an intermittent signal appears in the actual signal, the EMD decomposition method will produce a Mode Mixing Problem. The Mode Mixing Problem causes the essential modal function to lose its physical meaning. In addition, the Mode Mixing Problem will also make the algorithm of Empirical Mode Decomposition unstable, and any disturbance may generate a new intrinsic mode function. In order to solve this problem, scholars have proposed the use of noise-assisted processing methods, Ensemble empirical mode decomposition (EEMD) and Complementary Ensemble Empirical Mode Decomposition (CEEMD). The white noise has been added to the original signal to change the extreme point distribution of the signal in the EEMD method, while in the CEEMD method, a set of noise signals have been added to the original signal to change the extreme point distribution of the signal.

3. Line 55, “Consequently, parameters such as mean and variance also do not change over time.” In this sentence, I think it will be better to revise “parameters” as “statistical parameters”.

Response: *Thank you for your comment. It has been modified in the revised manuscript.*

4. Lines 59-62, “This method can decompose the signal data of different frequencies step by step according to the characteristics of the data and obtain several periodic and trending signals orthogonal to each other, which can decompose the stronger nonlinear and non-stationary signals into weaker nonlinear and non-stationary signals”. This sentence needs to make some corrections. As we know, the IMFs are orthogonal components, but the trending component is not orthogonal to any IMF component. Therefore, the above descriptions are not accurate. Besides, the sentence of “which can decompose the stronger nonlinear and non-stationary signals into weaker nonlinear and non-stationary signals” is ambiguous and makes no sense. Accurately, the EMD technique decomposes a non-stationary time series into several stationary subcomponent and a trend. But it is not easy to say the nonlinearity becomes weaker. So, I suggest the authors to make the sentence more accurate.

Response: *Thank you for the valuable criticism. We modified these sentences in the revised manuscript. “This method can decompose the signal data of different frequencies step by step according to the characteristics of the data and obtain several periodic and trending signals orthogonal to each other, which can decompose the stronger nonlinear and non-stationary signals. The EMD method is powerful and adaptive in analyzing nonlinear and non-stationary data sets. It provides an effective approach for decomposing a signal into a collection of so-called intrinsic mode functions (IMFs), which can be treated as empirical basis functions (Duan et al., 2016).”*

5. Lines 117-119, “The purpose of this study is to combine the EEMD algorithm and the CEEMD decomposition algorithm respectively with the BP neural network algorithm to establish a new prediction model, an improved hybrid EMD-BPNN model.” Accurately, the models of EEMD-BPNN and CEEMD-BPNN themselves are not new. Various works about

this models in different problems have already carried out in the last ten years. Therefore, I suggest the authors not to over emphasis “new” or “improved” here. Just simply describe them as “hybrid models”.

***Response:** Thank you for the suggestion. We modified these statements in the revised manuscript. “The purpose of this study is to combine the EEMD algorithm and the CEEMD decomposition algorithm respectively with the BP neural network algorithm to establish a prediction model, a hybrid EMD-BPNN model.”*

6. Lines 294-295, “This paper presents a novel SST predicting method based on the hybrid improved EMD algorithms and BP neural network method to process the SST data with strong nonlinearity and non-stationarity.” I suggest the authors to delete the word of “novel” here (and the same in the highlight part). Because the hybrid models have already explored extensively in various prediction problems. Besides, the authors argue that “the SST data with strong nonlinearity and non-stationarity.”, what is the standard of weak or strong nonlinearity and non-stationarity? Therefore, this sentence need to be corrected.

***Response:** Thank you for the suggestion. We modified these statements in the revised manuscript. “This paper presents an SST predicting method based on the hybrid EMD algorithms and BP neural network method to process the SST data with nonlinearity and non-stationarity.”*

References:

- Wu Z, Schneider E K, Kirtman B P, et al. The modulated annual cycle: an alternative reference frame for climate anomalies[J]. *Climate Dynamics*, 2008, 31(7-8): 823-841.
- Wu Z, Huang N E. Ensemble empirical mode decomposition: a noise-assisted data analysis method[J]. *Advances in adaptive data analysis*, 2009, 1(01): 1-41.
- Duan W, Huang L, Han Y, et al. A hybrid EMD-AR model for nonlinear and non-stationary wave forecasting[J]. *Journal of Zhejiang University-SCIENCE A*, 2016, 17(2): 115-129.

Hybrid improved EMD-BPNN model for the prediction of sea surface temperature

Zhiyuan Wu^{a,b,c}, Changbo Jiang^{a,c,*}, Mack Conde^d, Bin Deng^{a,c}, Jie Chen^{a,c}

a. School of Hydraulic Engineering, Changsha University of Science & Technology, Changsha, 410004, China;

b. School for Marine Science and Technology, University of Massachusetts Dartmouth, New Bedford, MA 02744, USA;

c. Key Laboratory of Water-Sediment Sciences and Water Disaster Prevention of Hunan Province, Changsha, 410004, China;

d. Department of Mathematics, University of Massachusetts Dartmouth, North Dartmouth, MA 02747, USA.

Highlights

- A novel SST predicting method based on the hybrid ~~improved~~-EMD algorithms and BP neural network method are proposed in this paper.
- SST prediction results based on the hybrid EEMD-BPNN and CEEMD-BPNN models are compared and discussed.
- Cases study of SST in the North Pacific shows that the proposed hybrid CEEMD-BPNN model can effectively predict the time-series SST.

Abstract: Sea surface temperature (SST) is the major factor that affects the ocean-atmosphere interaction, and in turn the accurate prediction of SST is the key to ocean dynamic prediction. In this paper, an SST predicting method based on ~~improved~~-empirical mode decomposition (EMD) algorithms and back-propagation neural network (BPNN) is proposed. Two different EMD algorithms have been applied extensively for analyzing time-series SST data and some nonlinear stochastic signals. Ensemble empirical mode decomposition (EEMD) algorithm and Complementary Ensemble Empirical Mode Decomposition (CEEMD) algorithm are two improved algorithms of EMD, which can effectively handle the mode-mixing problem and decompose the original data into more stationary signals with different frequencies. Each Intrinsic Mode Function (IMF) has been taken as an input data to the back-propagation neural network model. The final predicted SST data is obtained by aggregating the predicted data of individual IMF. A case study, of the monthly mean sea surface temperature anomaly (SSTA) in the northeastern region of the North Pacific, shows that the proposed hybrid CEEMD-BPNN model is much more accurate than the hybrid EEMD-BPNN model, and the prediction accuracy based on BP neural network is improved by the CEEMD method. Statistical analysis of the case study demonstrates that applying the proposed hybrid CEEMD-BPNN model

30 is effective for the SST prediction.

31

32 **Keywords.**

33 Sea Surface Temperature; Back-Propagation Neural Network; Empirical Mode Decomposition; Prediction;
34 Machine Learning Algorithms.

35

36 **1 Introduction**

37 The Sea Surface Temperature (SST) is a main factor in the interaction between the ocean and the
38 atmosphere (Wiedermann et al., 2017; He et al., 2017; Wu et al., 2019a), and it characterizes the combined
39 results of ocean heat (Buckley et al., 2014; Griffies et al., 2015; Wu et al., 2019b), dynamic processes
40 (Takakura et al., 2018). It is a very important parameter for climate change and ocean dynamics process,
41 reflects sea-air heat and water vapor exchange. Small changes in sea temperature can have a huge impact on
42 the global climate. The well-known El Niño and La Niña phenomena are caused by abnormal changes in SST
43 (Chen et al., 2016a; Zheng et al., 2016).

44 Therefore, scholars have begun to observe the SST in recent years, the observation of the SST is
45 important (Kumar et al., 2017; Sukresno et al., 2018). Accurate observation and effective prediction of the
46 SST are very important (Hudson et al., 2010). Predicting the SST in advance can enable people to take
47 appropriate measures to reduce the impact on daily life and reduce unnecessary losses. However, due to the
48 high randomness of the monthly mean sea surface temperature anomaly (SSTA), the nonlinear and non-
49 stationary characteristics are obvious. At present, there is no clear and feasible method with high accuracy to
50 effectively predict the SST (Zhu et al., 2015; Chen et al., 2016b; Khan et al., 2017).

51 In mathematics and science, a nonlinear system is a system in which the change of the output is not
52 proportional to the change of the input. Nonlinear dynamical systems, describing changes in variables over
53 time, may appear chaotic, unpredictable, or counterintuitive, contrasting with much simpler linear systems.
54 A stationary process is a stochastic process whose unconditional joint probability distribution does not change
55 when shifted in time. Consequently, statistical parameters such as mean and variance also do not change over
56 time. The variation of SST is a deterministic non-linear dynamic system and a non-stationary time series data.
57 ~~The observation sequence at a certain point contains not only the information of this point, but also the~~
58 ~~information of other relevant points.~~ Empirical Mode Decomposition (EMD) is a state-of-the-art signal
59 processing method proposed by Huang et al. (1998). This method can decompose the signal data of different

60 frequencies step by step according to the characteristics of the data and obtain several periodic and trending
61 signals orthogonal to each other, ~~which the method~~ can decompose the stronger nonlinear and non-stationary
62 signals ~~into weaker nonlinear and non-stationary signals~~ (Wang et al., 2015; Amezquita-Sanchez and
63 Adeli, 2015; Wang et al., 2016; Kim and Cho, 2016). The empirical mode decomposition (EMD) method is
64 powerful and adaptive in analyzing nonlinear and non-stationary data sets. It provides an effective approach
65 for decomposing a signal into a collection of so-called intrinsic mode functions (IMFs), which can be treated
66 as empirical basis functions (Duan et al., 2016). However, there were some problems of the EMD method,
67 such as mode mixing (Huang and Wu, 2008; Wu et al., 2008; Wu and Huang, 2009).

68 Once an intermittent signal appears in the actual signal, the EMD decomposition method will produce
69 a Mode Mixing Problem. The Mode Mixing Problem causes the essential modal function to lose its physical
70 meaning. In addition, the Mode Mixing Problem will also make the algorithm of Empirical Mode
71 Decomposition unstable, and any disturbance may generate a new intrinsic mode function. In order to solve
72 this problem, scholars have proposed the use of noise-assisted processing methods, Ensemble empirical mode
73 decomposition (EEMD) and Complementary Ensemble Empirical Mode Decomposition (CEEMD). The
74 white noise has been added to the original signal to change the extreme point distribution of the signal in the
75 EEMD method, while in the CEEMD method, a set of noise signals have been added to the original signal to
76 change the extreme point distribution of the signal.

77 To solve this problem, Wu and Huang (2009) proposed the Ensemble Empirical Mode Decomposition
78 (EEMD) method by adding different white noise in each ensemble member to suppress mode mixing. Yeh et
79 al. (2010) added two opposite-signal white noises to the time-series data sequence, and proposed an improved
80 algorithm for EEMD, Complete Ensemble Empirical Mode Decomposition (CEEMD). The decomposition
81 effect is equivalent to EEMD, and the reconstruction error caused by adding white noise is reduced (Tang et
82 al., 2015). At present, the EMD model and its improved algorithms had been widely used in many fields on
83 ocean science, such as storm surge and sea level rise (Wu et al., 2011; Lee, 2013; Ezer and Atkinson, 2014),
84 tidal amplitude (Cheng et al., 2017; Pan et al., 2018) and wave height (Duan et al., 2016; Sadeghifar et al.,
85 2017; López et al., 2017). These studies and applications reflected that the EMD model and its improved
86 algorithms can effectively reduce the non-stationarity of the time-series data, which helps further analysis
87 and processing.

88 For nonlinear prediction, the more commonly used methods are curve fitting (Motulsky and Ransnas,
89 1987), gray-box model (Pearson and Pottmann, 2000), homogenization function model (Monteiro et al.,

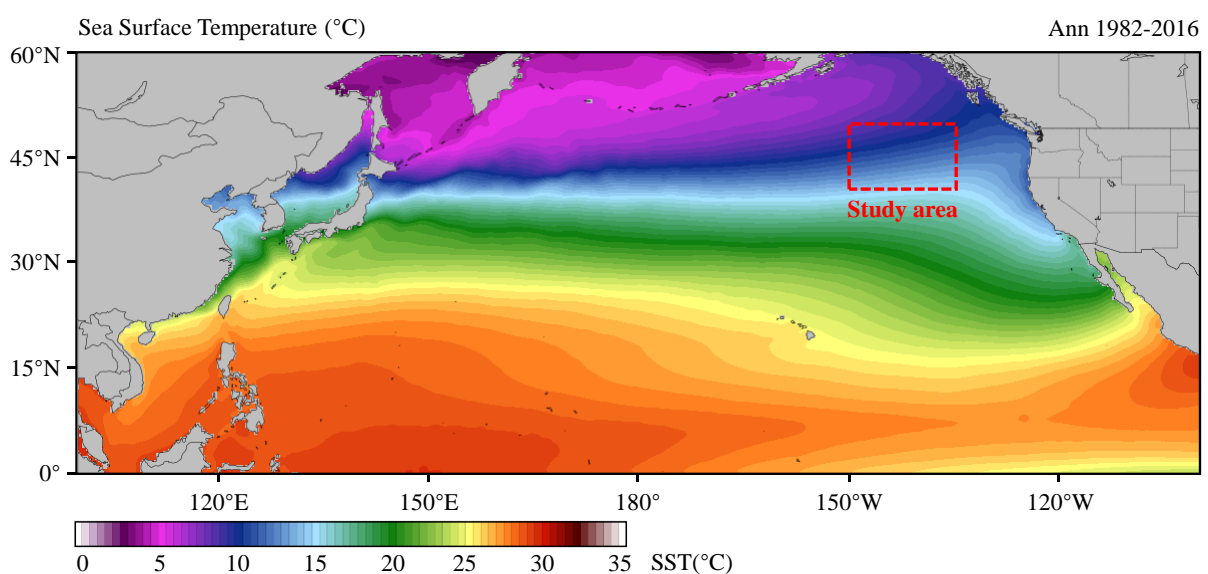
90 2008), neural network (Deo et al., 2001; Wang et al, 2015; Kim et al., 2016) and so on. Among them, Back-
91 Propagation Neural Network (BPNN) (Lee, 2004; Jain and Deo, 2006; Savitha and Al, 2017; Wang et al.,
92 2018) has certain advantages in dealing with nonlinear problems, it is a basic machine learning algorithm
93 and its principle is simple and operability is strong, so in ocean science and engineering it has been widely
94 used.

95 In view of non-stationary and nonlinear monthly mean SST, the EEMD, CEEMD and BP neural network
96 will be used here to study how to improve the accuracy of SST prediction. The ~~improved~~ hybrid EMD-BPNN
97 models will be established for the prediction of SSTA in the northeastern region of the Pacific Ocean.

98
99

100 2 Data collection

101 The SST time-series data in this study is from NOAA Optimum Interpolation Sea Surface Temperature
102 (OISST) official website (Reynolds et al., 2007; Banzon et al., 2016; [https://www.ncdc.noaa.gov/oisst/data-
103 access](https://www.ncdc.noaa.gov/oisst/data-access)). The NOAA 1/4°daily OISST is an analysis constructed by combining observations from different
104 platforms (satellites, ships, buoys) on a regular global grid. There are two kinds of OISST, named after the
105 relevant satellite SST sensors. These are the Advanced Very High Resolution Radiometer (AVHRR) and
106 Advanced Microwave Scanning Radiometer on the Earth Observing System (AMSR-E); the AVHRR dataset
107 is used in this study. The average annual sea surface temperature in North Pacific (0°N-60°N, 100°E-100°W)
108 ~~from during~~ January 1982 to December 2016 is shown in Fig.1.



109
110

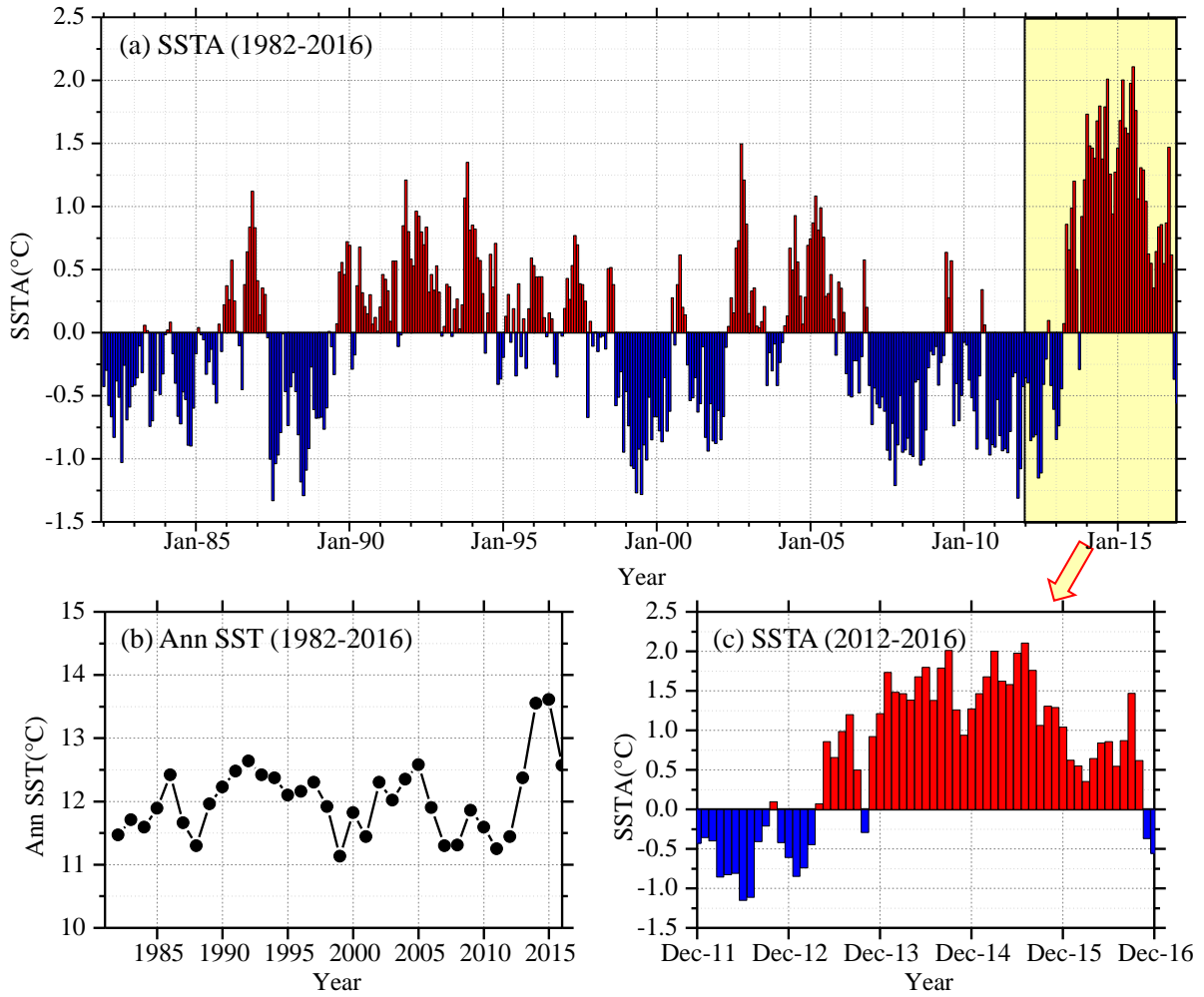
Fig.1 Average annual sea surface temperature in North Pacific during Jan 1982 to Dec 2016 (35-years).

111

112 It has been shown that the sea surface temperature anomaly in the northeastern Pacific in the ten years
113 2006-2016 was 2.0°C warmer than in the previous ten years 1996-2006. It had been shown that the sea
114 surface temperature anomaly in the northeastern Pacific is much hotter 2.0 °C than that in previous years
115 from the observations in recent ten years (2006-2016). Previous studies (Bond et al., 2015) showed that in
116 the spring and summer of 2014, the high SST area of the northeastern Pacific had expanded to coastal ocean
117 waters, which affected the weather in coastal areas and the lives of fishermen, and even affected the
118 temperature in Washington, USA, causing interference to daily life.~~the daily life had been caused~~
119 ~~interference.~~

120 In this study, we select the northeastern region of the North Pacific Ocean (in Fig.1, 40°N-50°N, 150°W-
121 135°W) to measure sea surface temperature. The time-series data of SST for the study area from January
122 1982 to December 2016 with a data length of 420 months was obtained from OISST-V2 (Fig. 2). The monthly
123 mean sea surface temperature anomaly (SSTA) was used in the analysis and calculation. As shown in Fig.
124 2(a), it can be found the overall time-series data is very messy, nonlinear and random from the perspective
125 of the image.

126



127

128 **Fig.2** The time-series of sea surface temperature in the study area. (a) SSTA anomaly (1982-2016, 35 years);
 129 (b) Annual SSTA (1982-2016, 35 years); (c) SSTA anomaly (2012-2016, 5 years).

130

131 3 Decomposition of SSTA

132 The purpose of this study is to combine the EEMD algorithm and the CEEMD decomposition algorithm
 133 respectively with the BP neural network algorithm to establish a **new** prediction model, an **improved** hybrid
 134 EMD-BPNN model. The EEMD and CEEMD algorithms are performed on the monthly mean SSTA data to
 135 obtain a series of intrinsic mode functions (IMFi). Each IMFi is predicted by a BP neural network and then
 136 each IMFi is reconstructed to obtain the predicted value of SSTA.

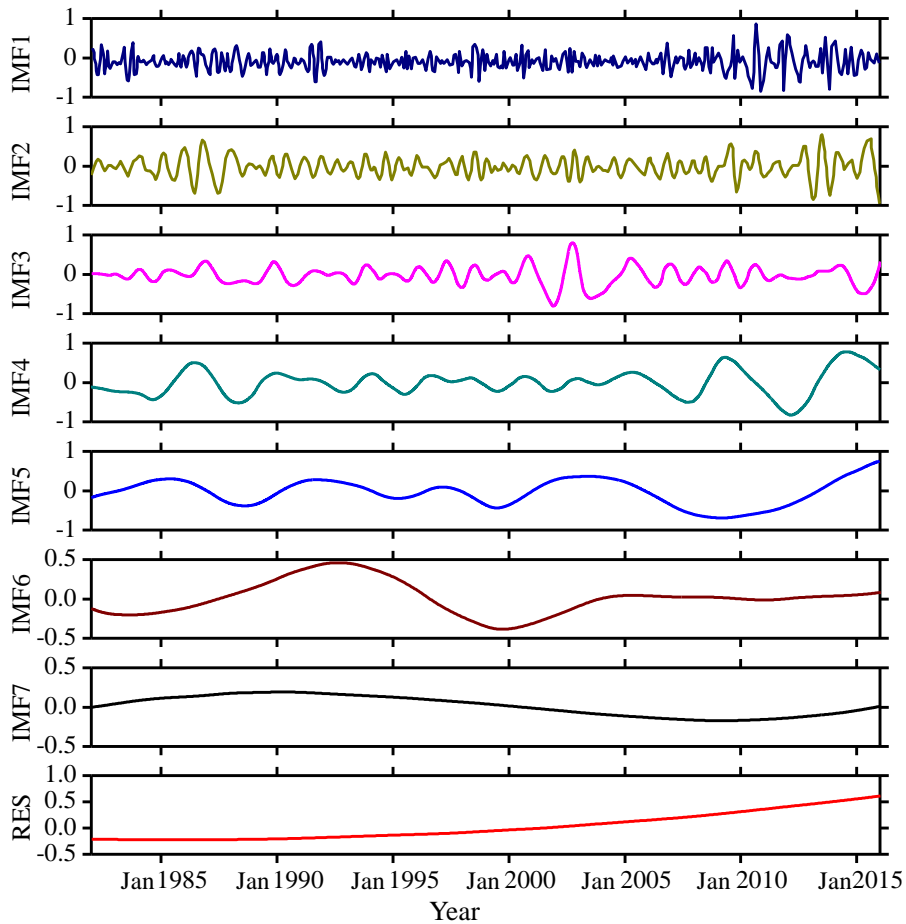
137 3.1 Decomposition by the EEMD algorithm

138 The SSTA in Fig. 2(a) has been decomposed based on the ensemble empirical mode decomposition
 139 (EEMD algorithm), and seven IMF components and a residual component RES (Residue) are obtained as
 140 shown in Fig. 3.

141 It can be seen from Fig. 3 that the first three intrinsic mode function components IMF1, IMF2, and IMF3
 142 still exhibit strong nonlinearity and non-stationarity. The IMF4 to IMF7 and the final trend term RES have
 143 some periodicity and relatively regular volatility, and the non-stationary and nonlinear properties are less
 144 than the first three components. The trend term RES reflects that the overall trend of SSTA has gradually
 145 increased since 1982. As the non-stationarity of each IMF $_i$ is gradually reduced, the EEMD algorithm will
 146 reduce the influence of non-stationarity on prediction. The absolute error (ERR) of the decomposition can
 147 be calculated by the following Formula (1).

$$148 \quad a(t) = \left| S(t) - \left[\sum_{i=1}^7 I_i(t) + R(t) \right] \right| \quad (1)$$

149 where, $a(t)$ is the absolute error (ERR), $S(t)$ the original SSTA observation data, $I_i(t)$ the i -th component
 150 of the IMF (IMF $_i$), and $R(t)$ the trend term (RES).
 151



152
 153 **Fig.3** IMF components and the trend item RES of monthly mean SSTA over the study area based on the
 154 EEMD algorithm during 1982-2016.

155
156
157
158
159
160
161
162
163
164
165
166
167
168
169
170
171
172
173
174

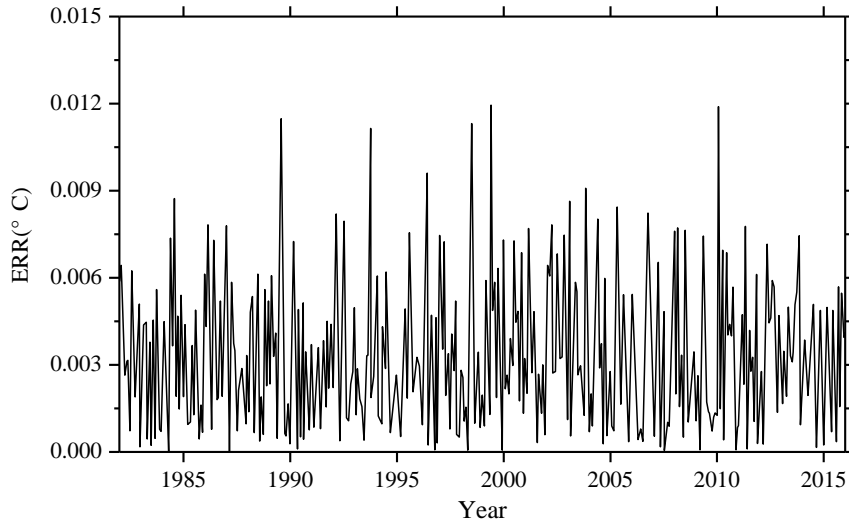
It can be seen from Fig. 3 that the first three intrinsic mode function components IMF1, IMF2, and IMF3 still exhibit strong nonlinearity and non-stationarity. The IMF4 to IMF7 and the final trend term RES have some periodicity and relatively regular fluctuation, and the non-stationary and nonlinear properties are less than the first three components. The trend term RES reflects that the overall trend of SSTA has gradually increased since 1982. As the non-stationarity of each IMF_i is gradually reduced, the EEMD algorithm will reduce the influence of non-stationarity on prediction. The absolute error (ERR) of the decomposition can be calculated by the following Formula (1).

$$a(t) = \left| S(t) - \left[\sum_{i=1}^7 I_i(t) + R(t) \right] \right| \tag{1}$$

where, $a(t)$ is the absolute error (ERR), $S(t)$ the original SSTA observation data, $I_i(t)$ the i -th component of the IMF (IMF _{i}), and $R(t)$ the trend term (RES).

The absolute error (ERR) based on the EEMD algorithm ~~was~~ is shown in Fig. 4. It can be seen from the figure that the ERR of 420 months after decomposition is basically below 0.01 °C, and the ERR ~~–~~exceeds 0.01 °C in five months: June 1989, September 1993, July 1998, May 1999 and March 2010.

In addition to June 1989, the other four monthly data with a large ERR occurred during the El Niño period. The maximum error is in March 2010, the actual value is -0.1204 °C, the result based on EEMD algorithm is -0.1325 °C, the ERR of decomposition is 0.0121 °C; the minimum error, in April 1987, is 1.73×10^{-5} °C. The overall mean ERR based on the EEMD algorithm is 0.0035 °C and the order of magnitude is 10^{-3} .



175

176 **Fig. 4** The ERR of monthly mean SSTA over the study area based on the EEMD algorithm during 1982-2016.

177

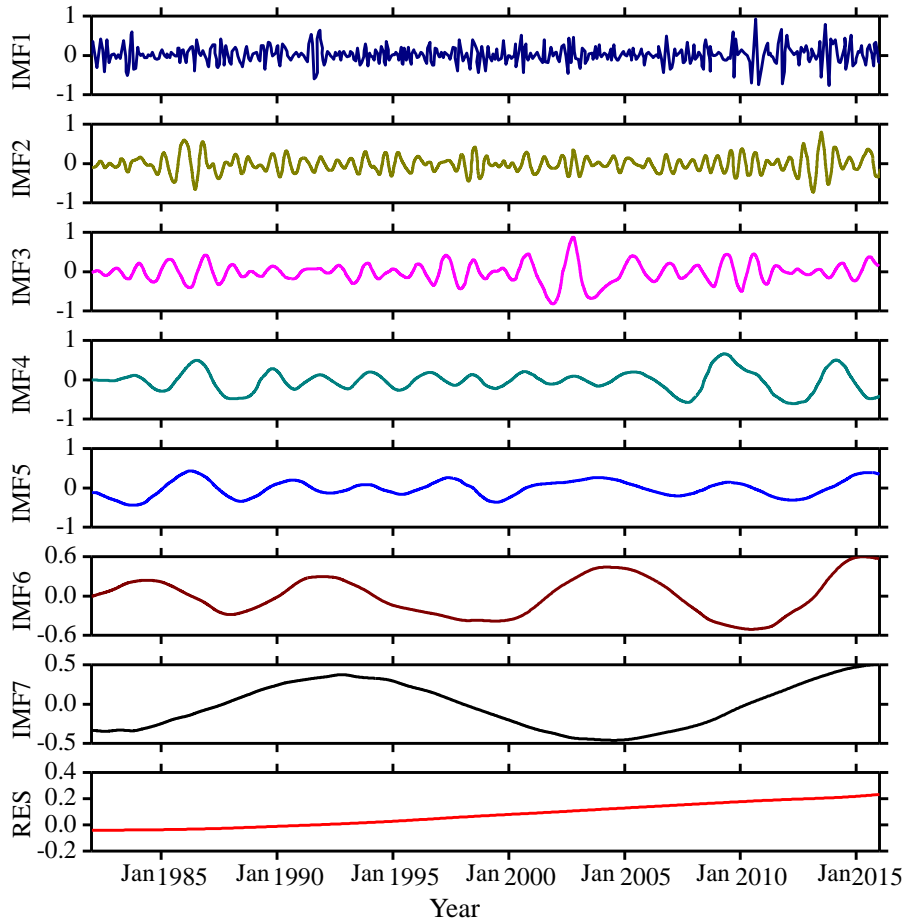
178 ~~In addition to June 1989, the other four monthly data with a large ERR occurred during the El Niño~~
 179 ~~period. The maximum error is in March 2010, the actual value is $-0.1204\text{ }^{\circ}\text{C}$, the result based on EEMD~~
 180 ~~algorithm is $-0.1325\text{ }^{\circ}\text{C}$, the ERR of decomposition is $0.0121\text{ }^{\circ}\text{C}$; the minimum error is in April 1987, which~~
 181 ~~is $1.73 \times 10^{-5}\text{ }^{\circ}\text{C}$. The overall mean ERR based on EEMD algorithm is $0.0035\text{ }^{\circ}\text{C}$ and the order of magnitude~~
 182 ~~is 10^{-3} .~~

183

184 **3.2 Decomposition by the CEEMD algorithm**

185 The SSTA has been decomposed based on the complementary ensemble empirical mode decomposition
 186 (CEEMD algorithm) and seven IMF components and a residual component RES (Residue) are obtained as
 187 shown in Fig. 5. It can be seen when comparing the decomposition results based on EEMD and CEEMD
 188 algorithms that although the mode components decomposed by CEEMD algorithm are different from the
 189 corresponding results decomposed by EEMD, the nonlinearities and non-stationarities of the eight modes
 190 decomposed by the two decomposition algorithms are gradually decreasing, and the final trend term RES is
 191 an upward trend. Both decomposition algorithms confirm the characteristic of a gradual increase ~~infer~~ the
 192 overall trend of the data series.

193



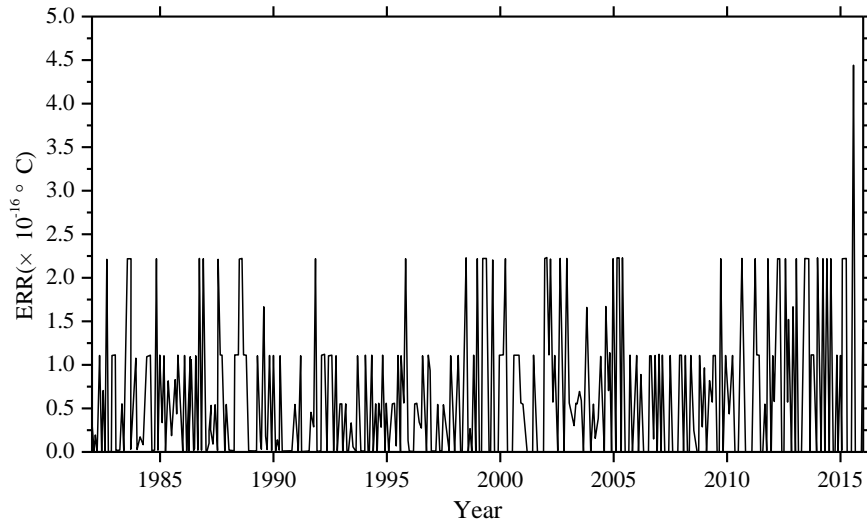
194

195 **Fig.5** IMF components and the trend item RES of monthly mean SSTA over the study area based on the
 196 CEEMD algorithm during 1982-2016.

197

198 The absolute error (ERR) obtained based on the CEEMD algorithm is shown in Fig. 6. It can be seen
 199 from the figure that the ERR of 420 months data after decomposition is less than $5 \times 10^{-16} \text{ }^\circ\text{C}$, and the accuracy
 200 is very better. The maximum error is $4.48 \times 10^{-16} \text{ }^\circ\text{C}$ in March 2016; the minimum error is zero. The overall
 201 mean ERR based on CEEMD algorithm is $6.10 \times 10^{-17} \text{ }^\circ\text{C}$ and the order of magnitude is 10^{-17} . By comparing
 202 the results and errors of the above two decomposition algorithms, it can be seen that the error based on the
 203 improved algorithm (CEEMD) is much smaller than the error based on EEMD algorithm. Because more
 204 white noise with the opposite sign had been added in CEEMD algorithm, the reconstruction error caused
 205 by the white noise has been reduced over it in EEMD algorithm.

206



207

208 **Fig. 6** The ERR of monthly mean SSTA over the study area based on the CEEMD algorithm during 1982-
 209 2016.

210

211 ~~The absolute error (ERR) obtained based on the CEEMD algorithm is shown in Fig. 6. It can be seen~~
 212 ~~from the figure that the ERR of 420 months data after decomposition is less than $5 \times 10^{-16} \text{ }^\circ\text{C}$, and the accuracy~~
 213 ~~is very better. The maximum error is $4.48 \times 10^{-16} \text{ }^\circ\text{C}$ in March 2016; the minimum error is zero. The overall~~
 214 ~~mean ERR based on CEEMD algorithm is $6.10 \times 10^{-17} \text{ }^\circ\text{C}$ and the order of magnitude is 10^{-17} . By comparing~~
 215 ~~the results and errors of the above two decomposition algorithms, it can be seen that the error based on the~~
 216 ~~improved algorithm (CEEMD) is much smaller than the error based on EEMD algorithm. This is because~~
 217 ~~more white noise in CEEMD algorithm had been added than that in EEMD algorithm, so reducing the~~
 218 ~~reconstruction error caused by white noise when the decomposition effect is equivalent to EEMD algorithm.~~

219

220 4 SSTA prediction model

221 4.1 The BP neural network

222 Artificial Neural Network (ANN) is an information processing approach based on the biological neural
 223 network (López et al., 2015; Kim et al., 2016). In theory, ANN can simulate any complex nonlinear
 224 relationship through nonlinear units (neurons) and has been widely used in the prediction area, such as wave
 225 height and storm surge. The most basic structure of ANN consists of input layers, hidden layers and output
 226 layers. One of the most widely used ANN models is the back propagation neural network (BPNN, Wang et
 227 al., 2018) algorithm based on the BP algorithm.

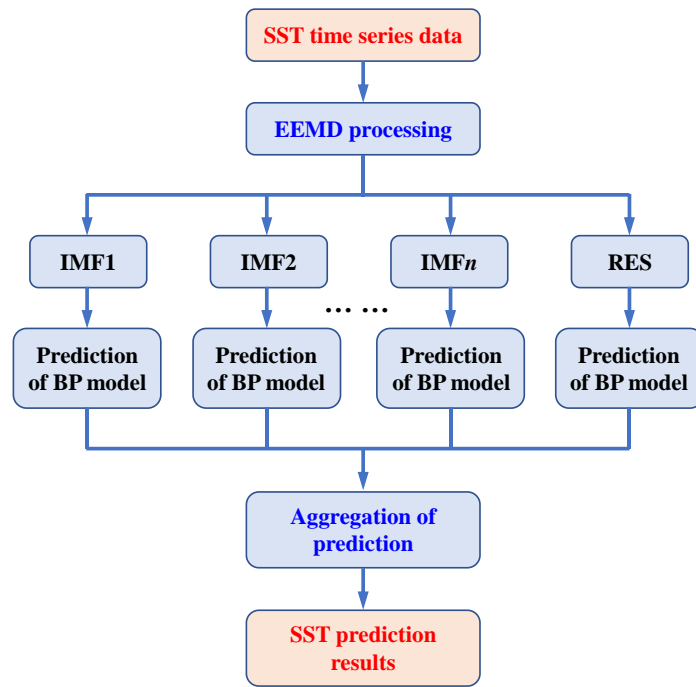
228 The BPNN algorithm is a multi-layer feedforward network trained according to the error back
229 propagation algorithm and is one of the most widely used deep learning algorithms. The BP network can be
230 used to learn and store a large number of mappings of input and output models without the need to publicly
231 describe the mathematical equations of these mapping relationships. The learning rule is to use the steepest
232 descent method. When applied to SST predicting, the input data are monthly mean SST in previous months
233 and the output data are predicted SST time-series data. The desired data for comparison is the observed actual
234 SST.

235

236 **4.2 SSTA prediction model based on hybrid improved EMD-BPNN algorithm**

237 The proposed monthly mean sea surface temperature anomaly (SSTA) predicting model includes three
238 steps as follows. First, original SST datasets are decomposed into certain more stationary signals with
239 different frequencies by EEMD. Second, the BP neural network is used to predict each IMF and the residue
240 RES. A rolling forecasting process is studied. The prediction is made using the previous data for one step
241 ahead. Finally, the prediction results of each IMF and the residue RES are aggregated to obtain the final SST
242 prediction results. The flowchart of the SST prediction model based on hybrid improved empirical mode
243 decomposition algorithm (improved EMD algorithm) and back-propagation neural network (BPNN) is shown
244 in Fig. 7. The SST prediction model has been abbreviated as a hybrid improved EMD-BPNN model in the
245 following article.

246



247

248 **Fig.7** The flowchart of SST prediction model based on hybrid improved empirical mode decomposition
 249 algorithm (improved EMD algorithm) and back-propagation neural network (BPNN).

250

251

252 **5 Case study: SSTA prediction based on the hybrid improved EMD-BPNN models**

253 In order to study the effects of the two improved EMD algorithms (EEMD and CEEMD) on the
 254 prediction results, and to analyze the prediction ability of BP neural network, the following experiments were
 255 carried out. Predict SSTA results in 2017 and analyze the prediction abilities of different mode decomposition
 256 data based on EEMD and CEEMD algorithms. The experiment content is as follows: the BP neural network
 257 is trained with the decomposition data of each mode from 1982 to 2016, and the SSTA in 2017 is predicted
 258 by the trained neural network, and the observation results of 12 months in 2017 ~~areis~~ used to compare and
 259 analyze with the prediction results.

260 Since the nonlinearity of the IMF1 to IMF3 is still relatively strong, a three-layer BP neural network
 261 structure has been chosen and independently analyze and predict each month. For the IMF4 and subsequent
 262 modes, since the nonlinearity and non-stationarity have been degraded relative to the first three modes, a BP
 263 neural network with 12 nodes at input layer and output layer has been used to train and predict SSTA.

264 The prediction results of each mode decomposition component based on the EEMD algorithm are shown
 265 in Fig. 8. The absolute errors of the predicted value and the actual value are shown in Table 1. ~~Root-mean~~

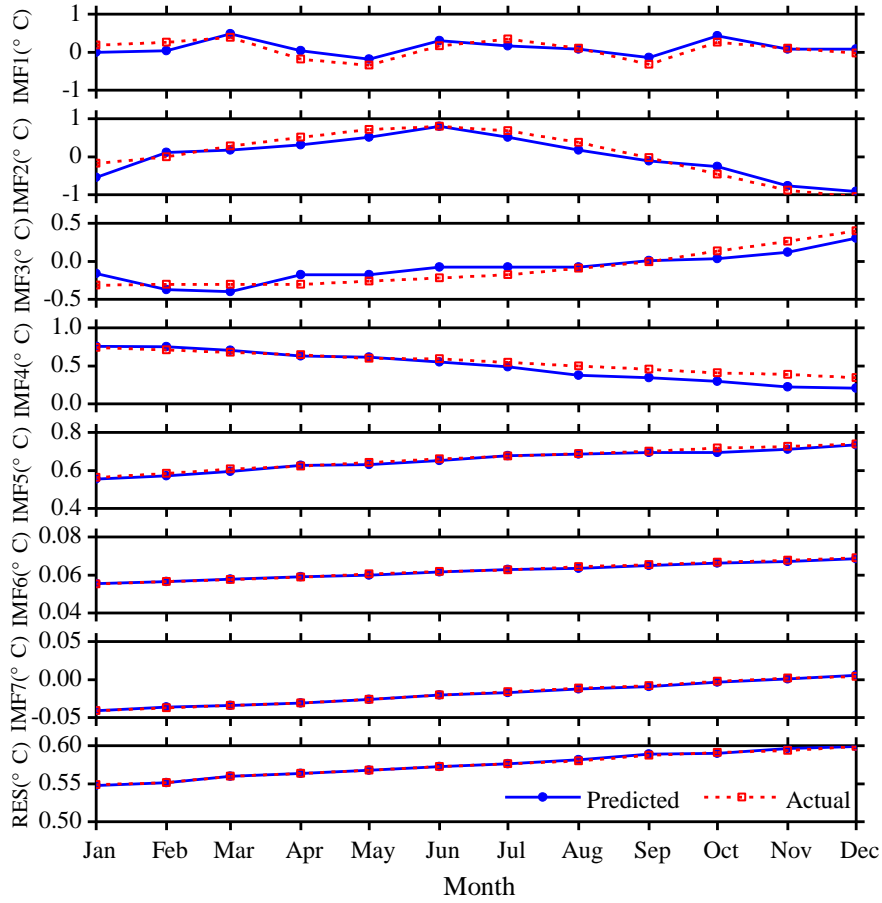
266 square error (RMSE) is used as metrics to access the performance of the two different models.

$$267 \quad \text{RMSE} = \sqrt{\frac{1}{N} \sum_{n=1}^N (x_n - y_n)^2} \quad (2)$$

268 where, x_n and y_n are the observed and the predicted values respectively, N is the number of data used for
269 the performance evaluation. Results are shown in Table 1.

270 It can be seen from Fig. 8 and Table 1 that the maximum absolute error (Max ERR) of the first
271 decomposition component IMF1 based on the hybrid EEMD-BPNN model is 0.2197 °C in January. The
272 minimum absolute error (Min ERR) is 0.0014 °C, which is in August. The prediction ability of the second
273 mode decomposition component IMF2 is roughly equivalent to the IMF1, and the mean absolute error (Mean
274 ERR) of the first three intrinsic mode function components IMF1, IMF2, and IMF3 are between 0.10 °C and
275 0.15 °C. The mean absolute errors of the IMF4 and IMF5 are 0.0663 °C and 0.0089 °C, respectively, and the
276 prediction accuracy based on the hybrid EEMD-BPNN model is roughly equivalent to the decomposition
277 accuracy of the EEMD algorithm. The prediction errors of the last two intrinsic mode function components
278 and the residue RES are on the order of 10^{-4} . It can be seen that as the nonlinearity and non-stationarity of
279 the series data decreases, the error of the prediction results becomes smaller and smaller.

280



281
 282 **Fig. 8** SSTA prediction results based on the hybrid EEMD-BPNN model of each individual component in
 283 2017.

284
 285 Root mean square error (RMSE) is used as metrics to access the performance of the two different models.

$$286 \quad \text{RMSE} = \sqrt{\frac{1}{N} \sum_{n=1}^N (x_n - y_n)^2} \quad (2)$$

287 where, x_n and y_n are the observed and the predicted values respectively, N is the number of data used for
 288 the performance evaluation. Results are shown in Table 1.

289
 290 **Table 1.** The absolute errors ERRs of the SSTA prediction results of each individual component based on the
 291 hybrid EEMD-BPNN model (unit: °C).

	Max ERR	Min ERR	Mean ERR	RMSE
IMF1	0.2197	0.0014	0.1424	0.1486
IMF2	0.2166	0.0323	0.1297	0.1673
IMF3	0.1872	0.0051	0.1070	0.1245

IMF4	0.1602	1.6876869×10^{-4}	0.0663	0.0857
IMF5	0.0158	0.0010	0.0089	0.0104
IMF6	3.8778766×10^{-4}	1.9752×10^{-4}	2.7221×10^{-4}	0.0003
IMF7	5.2662×10^{-4}	1.6396387×10^{-4}	1.7917907×10^{-4}	0.0002
RES	5.4864859×10^{-4}	2.2312308×10^{-4}	2.4774766×10^{-4}	0.0002

292

293

294

295

296

297

298

299

300

301

302

It can be seen from Fig. 8 and Table 1 that the maximum absolute error (Max ERR) of the first decomposition component IMF1 based on the hybrid EEMD-BPNN model is 0.2197 °C in January. The minimum absolute error (Min ERR) is 0.0014 °C, which is in August. The prediction ability of the second mode decomposition component IMF2 is roughly equivalent to the IMF1, and the mean absolute error (Mean ERR) of the first three intrinsic mode function components IMF1, IMF2, and IMF3 are between 0.10 °C and 0.15 °C. The mean absolute errors of the IMF4 and IMF5 are 0.0663 °C and 0.0089 °C, respectively, and the prediction accuracy based on the hybrid EEMD-BPNN model is roughly equivalent to the decomposition accuracy of the EEMD algorithm. The prediction errors of the last two intrinsic mode function components and the residue RES are on the order of 10^{-4} . It can be seen that as the nonlinearity and non-stationarity of the series data decreases, the error of the prediction results becomes smaller and smaller.

303

304

305

306

307

According to the same method, the eight mode components decomposed by CEEMD algorithm have been analyzed and predicted. The prediction results and error analysis have been shown in Fig. 9 and Table 2. It can be seen from Fig. 9 and Table 2 that the maximum error of the first decomposition component IMF1 based on the hybrid CEEMD-BPNN model is 0.1779 °C in May. The minimum error is 0.0068 °C, which is in June.

308

309

310

311

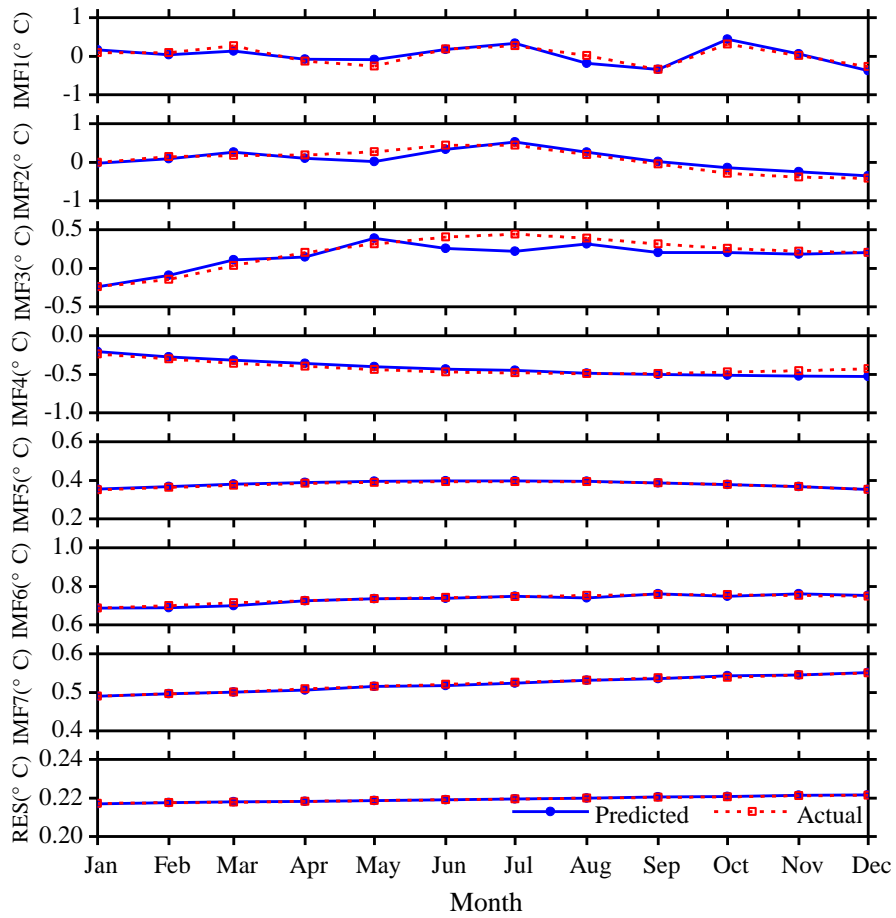
312

313

314

315

The prediction ability of the second mode decomposition component IMF2 is roughly equivalent to the IMF1. Except for the four months of May, September, October, and November, the accuracies of prediction results of other months are satisfactory. The prediction results of the first three intrinsic mode function components IMF1, IMF2, and IMF3 are basically the same as the actual data. In the prediction results of the fourth mode component IMF4, except for slight error in December, the prediction ability is better. The predicted results of the last three intrinsic mode function components IMF5, IMF6, IMF7 and the residue RES are basically consistent with the observation results.



316

317 **Fig. 9** SSTA prediction results based on the hybrid CEEMD-BPNN model of each individual component in

318 2017.

319 _____

320

321 **Table 2.** The absolute errors ERRs of the SSTA prediction results of each individual component based on the
 322 hybrid CEEMD-BPNN model (unit: °C).

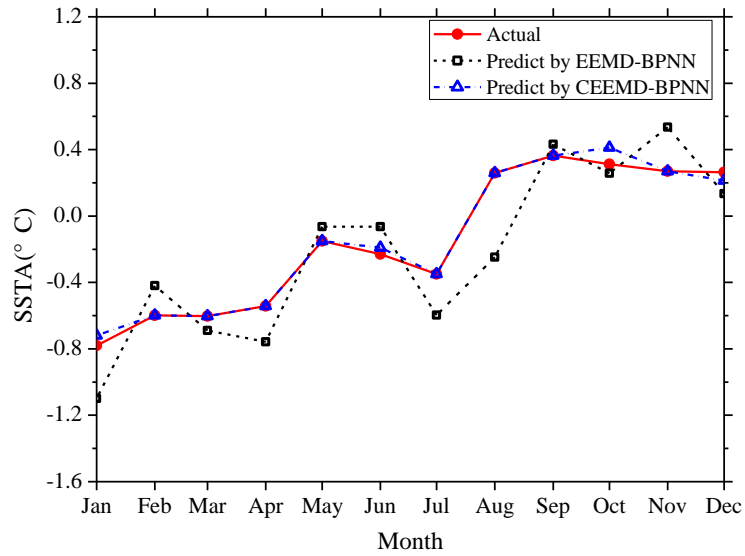
	Max ERR	Min ERR	Mean ERR	RMSE
IMF1	0.1779	0.0068	0.0827	0.0987
IMF2	0.1643	0.0413	0.0811	0.1124
IMF3	0.1521	0.0160	0.0713	0.1006
IMF4	0.0851	0.0211	0.0324	0.0427
IMF5	0.0052	8.7694×10^{-5}	0.0021	0.0029
IMF6	0.0103	5.7757748×10^{-5}	0.0043	0.0056
IMF7	0.0017	3.6036026×10^{-5}	9.1374×10^{-4}	0.0010
RES	3.0342×10^{-5}	2.0163×10^{-6}	1.1572×10^{-5}	1.5025017×10^{-5}

323

324 ~~The prediction ability of the second mode decomposition component IMF2 is roughly equivalent to the~~
 325 ~~IMF1. Except for the four months of May, September, October, and November, the accuracies of prediction~~
 326 ~~results of other months are satisfactory. The prediction results of the first three intrinsic mode function~~
 327 ~~components IMF1, IMF2, and IMF3 are basically the same as the actual data. In the prediction results of the~~
 328 ~~fourth mode component IMF4, except for slight error in December, the prediction ability is better. The~~
 329 ~~predicted results of the last three intrinsic mode function components IMF5, IMF6, IMF7 and the residue~~
 330 ~~RES are basically consistent with the observation results.~~

331 The prediction results of the monthly mean SSTA in 2017 are obtained by reconstructing the mode
 332 decomposition components (Fig. 10) and the absolute error (ERR) of prediction results has been shown in
 333 Table 3. It can be seen from the figure and table that the prediction results based on the EEMD-BPNN model
 334 have larger ERRs in January and August, exceeding 0.3 °C, and the accuracies of prediction results in other
 335 months are satisfactory (the ERR is less than 0.3). The prediction accuracy based on the CEEMD-BPNN
 336 model is satisfactory, except for the ERR exceeding 0.1 °C in October, and the prediction ability based on
 337 the CEEMD-BPNN model is generally better than that of the EEMD-BPNN model.

338



339
340 **Fig. 10** Monthly SSTA prediction results based on the hybrid improved EMD-BPNN models in 2017.

341
342

343 **Table 3.** The absolute errors ERRs of the SSTA prediction results based on the two different hybrid improved
344 EMD-BPNN models (unit: °C).

	EEMD-BPNN model	CEEMD-BPNN model		EEMD-BPNN model	CEEMD-BPNN model
Jan	0.3188	0.0623	Sep	0.0687	0.0132
Feb	0.1780	0.0103	Oct	0.0545	0.1607
Mar	0.0867	0.0063	Nov	0.2651	0.0101
Apr	0.2153	0.0137	Dec	0.1290	0.0183
May	0.0854	0.0102	Min ERR	0.0545	0.0063
Jun	0.1662	0.0224	Max ERR	0.5068	0.1607
Jul	0.2474	0.0077	Mean ERR	0.1935	0.0289
Aug	0.5068	0.0112	RMSE	0.2299	0.0512

345
346 The prediction values based on the CEEMD-BPNN model and the observation values at the significance
347 level of 0.001, the correlation coefficient reached 0.97Correlation coefficient between the prediction values
348 based on the CEEMD-BPNN model and observations is shown that the value of the correlation coefficient
349 that indicates a significance level of 0.001 and the correlation coefficient reached 0.97.; The result which
350 indicates that SSTA in 2017 had been predicted accurately by the CEEMD-BPNN model. As can be seen

351 from the above discussions, the ERR of decomposition components based on the EEMD and CEEMD
352 algorithms will affect the accuracy of the final prediction results. Table 3 shows that predicting results of the
353 hybrid CEEMD and BPNN model are ameliorated a lot as compared to the EEMD-BPNN direct predicting
354 model. This is because after CEEMD, the original unsteady and nonlinear data are changed into certain
355 components that have fixed frequency and periodicity. The CEEMD algorithm with less decomposition error
356 has less error in the final prediction results, which proves that the CEEMD method has more advantages in
357 data decomposition than the EEMD method. At the same time, we can find that the final prediction error of
358 the two prediction models mainly comes from the first three mode decomposition components, and the error
359 of the last five components has little effect on the accuracy of the final prediction results.

360

361 **6 Conclusions**

362 This paper presents a ~~novel~~ SST predicting method based on the hybrid ~~improved~~ EMD algorithms and
363 BP neural network method to process the SST data with ~~strong~~ nonlinearity and non-stationarity. Through
364 EEMD and CEEMD algorithms, SSTA time-series data are decomposed into different IMFs and a residue
365 RES. BP neural network is applied to predict individual IMFs and the residue RES. Final results can be
366 obtained by adding the predicting results of individual IMFs and RES.

367 In order to illustrate the effectiveness of the proposed approach, a case study was carried out. SSTA
368 ~~prediction~~ prediction results based on the hybrid EEMD-BPNN model and the hybrid CEEMD-BPNN model
369 are discussed respectively. In comparison, the proposed hybrid CEEMD-BPNN model is much better and its
370 prediction results are more accurate.

371 From the absolute error of the prediction results of each component IMF and the absolute error of the
372 predicted SSTA, the prediction error of SSTA mainly comes from the prediction of the first three mode
373 decomposition component (IMF1, IMF2 and IMF3), because the first three mode components still have
374 strong nonlinearity and non-stationarity. As the nonlinearity gradually decreases, the absolute error of the
375 prediction results gradually decreases.

376 SST prediction has been only preliminary carried out based on the two improved EMD algorithms and
377 BP neural network in this paper. The results show that the hybrid CEEMD-BPNN model is more accurate in
378 predicting SST. This work can provide a reference for predicting SST and El Niño in the future. In the follow-
379 up study, how to improve the forecast duration is the focus of this work.

380

381 **Acknowledgement**

382 This work was supported by National Natural Science Foundation of China (Grant Nos. 51809023,
383 51879015, 51839002, 51809021 and 51509023).

384

385 **References:**

386 Amezquita-Sanchez, J. P. and Adeli, H.: A new music-empirical wavelet transform methodology for time–
387 frequency analysis of noisy nonlinear and non-stationary signals, *Digit. Signal Process.*, 45, 55-68,
388 <https://doi.org/10.1016/j.dsp.2015.06.013>, 2015.

389 Banzon, V., Smith, T. M., Chin, T. M., Liu, C., and Hankins, W.: A long-term record of blended satellite and
390 in situ sea-surface temperature for climate monitoring, modeling and environmental studies, *Earth Syst.*
391 *Sci. Data*, 8, 165-176, <https://doi.org/10.5194/essd-8-165-2016>, 2016.

392 Bond, N. A., Cronin, M. F., Freeland, H., and Mantua N.: Causes and impacts of the 2014 warm anomaly in
393 the NE Pacific. *Geophys. Res. Lett.*, 42, 3414-3420, <https://doi.org/10.1002/2015GL063306>, 2015.

394 Buckley, M. W., Ponte, R. M., Forget, G., and Heimbach, P.: Low-frequency SST and upper-ocean heat
395 content variability in the North Atlantic, *J. Climate*, 27, 4996-5018, [https://doi.org/10.1175/JCLI-D-13-](https://doi.org/10.1175/JCLI-D-13-00316.1)
396 00316.1, 2014.

397 Chen, C., Cane, M. A., Henderson, N., Lee, D. E., Chapman, D., Kondrashov D., and Chekroun, M. D.:
398 Diversity, nonlinearity, seasonality, and memory effect in ENSO simulation and prediction using
399 empirical model reduction, *J. Climate*, 29: 1809-1830, <https://doi.org/10.1175/JCLI-D-15-0372.1>,
400 2016b.

401 Chen, Z., Wen, Z., Wu, R., Lin X., and Wang J.: Relative importance of tropical SST anomalies in maintaining
402 the Western North Pacific anomalous anticyclone during El Niño to La Niña transition years, *Clim.*
403 *Dynam.*, 46, 1027-1041, <https://doi.org/10.1007/s00382-015-2630-1>, 2016a.

404 Cheng, Y., Ezer, T., Atkinson, L. P., and Xu, Q.: Analysis of tidal amplitude changes using the EMD method,
405 *Cont. Shelf Res.*, 148: 44-52, <https://doi.org/10.1016/j.csr.2017.09.009>, 2017.

406 Deo, M. C., Jha, A., Chaphekar, A. S., and Ravikant, K.: Neural networks for wave forecasting, *Ocean Eng.*,
407 28: 889-898, [https://doi.org/10.1016/S0029-8018\(00\)00027-5](https://doi.org/10.1016/S0029-8018(00)00027-5), 2001.

408 Duan, W. Y., Han, Y., Huang, L. M., Zhao, B. B., and Wang, M. H.: A hybrid EMD-SVR model for the short-
409 term prediction of significant wave height, *Ocean Eng.*, 124, 54-73,
410 <https://doi.org/10.1016/j.oceaneng.2016.05.049>, 2016.

411 [Duan, W., Huang, L., Han Y., and Huang D.: A hybrid EMD-AR model for nonlinear and non-stationary](#)
412 [wave forecasting, J Zhejiang Univ-Sc A, 17\(2\): 115-129, <https://doi.org/10.1631/jzus.A1500164>, 2016.](#)

413 Ezer, T. and Atkinson, L. P.: Accelerated flooding along the US East Coast: on the impact of sea - level rise,
414 tides, storms, the Gulf Stream, and the North Atlantic oscillations, *Earths Future*, 2, 362-382,
415 <https://doi.org/10.1002/2014EF000252>, 2014.

416 Griffies, S. M., Winton, M., Anderson, W. G., Benson, R., Delworth, T. L., Dufour, C. O., Dunne, J. P.,
417 Goddard, P., Morrison, A. K., Rosati, A., Wittenberg, A. T., Yin, J., and Zhang, R.: Impacts on ocean
418 heat from transient mesoscale eddies in a hierarchy of climate models. *J. Climate*, 28, 952-977,
419 <https://doi.org/10.1175/JCLI-D-14-00353.1>, 2015.

420 He, J., Deser, C., and Soden, B. J.: Atmospheric and oceanic origins of tropical precipitation variability. *J.*
421 *Climate*, 30, 3197-3217, <https://doi.org/10.1175/JCLI-D-16-0714.1>, 2017.

422 Huang, N. E., Shen, Z., Long, S. R., Wu, M. C., Shih, H. H., Zheng, Q., Yen, N., Tung, C. C., and Liu, H. H.:
423 The empirical mode decomposition and the Hilbert spectrum for nonlinear and non-stationary time
424 series analysis, *P. Roy. Soc. A-Math. Phys.*, 454, 903-995. <https://doi.org/10.1098/rspa.1998.0193>, 1998.

425 Huang, N. E. and Wu, Z.: A review on Hilbert - Huang transform: Method and its applications to geophysical
426 studies, *Rev. Geophys.*, 46, RG2006, <https://doi.org/10.1029/2007RG000228>, 2008.

427 Hudson, D., Alves, O., Hendon, H. H., Wang, G.: The impact of atmospheric initialisation on seasonal
428 prediction of tropical Pacific SST, *Clim. Dynam.*, 36, 1155-1171, [https://doi.org/10.1007/s00382-010-](https://doi.org/10.1007/s00382-010-0763-9)
429 [0763-9](https://doi.org/10.1007/s00382-010-0763-9), 2011.

430 Jain, P. and Deo, M. C.: Neural networks in ocean engineering, *Ships Offshore Struc.*, 1, 25-35,
431 <https://doi.org/10.1533/saos.2004.0005>, 2006.

432 Khan, M. Z. K., Sharma, A., and Mehrotra, R.: Global seasonal precipitation forecasts using improved sea
433 surface temperature predictions, *J Geophys. Res. -Atmos.*, 122, 4773-4785,
434 <https://doi.org/10.1002/2016JD025953>, 2017,

435 Kim, Y., Kim, H., and Ahn, I. G.: A study on the fatigue damage model for Gaussian wideband process of
436 two peaks by an artificial neural network, *Ocean Eng.*, 111, 310-322,
437 <https://doi.org/10.1016/j.oceaneng.2015.11.008>, 2016.

438 Kumar, M., Parmar, C., Chaudhary, V., Kumar, A., and SST-1 team.: Observation of plasma shift in SST-1
439 using optical imaging diagnostics, *J Phys. Conf. Ser.*, 823, 012056, [https://doi.org/10.1088/1742-](https://doi.org/10.1088/1742-6596/823/1/012056)
440 [6596/823/1/012056](https://doi.org/10.1088/1742-6596/823/1/012056), 2017.

441 Lee, H. S.: Estimation of extreme sea levels along the Bangladesh coast due to storm surge and sea level rise
442 using EEMD and EVA, *J Geophys. Res.-Oceans*, 118, 4273-4285, <https://doi.org/10.1002/jgrc.20310>,
443 2013,

444 Lee, T. L.: Back-propagation neural network for long-term tidal predictions, *Ocean Eng.*, 31, 225-238,
445 [https://doi.org/10.1016/S0029-8018\(03\)00115-X](https://doi.org/10.1016/S0029-8018(03)00115-X), 2004.

446 López, I., Aragonés, L., Villacampa, Y., and Serra, J. C.: Neural network for determining the characteristic
447 points of the bars, *Ocean Eng.*, 136: 141-151, <https://doi.org/10.1016/j.oceaneng.2017.03.033>, 2017.

448 Monteiro, E., Yvonnet, J., He, Q. C.: Computational homogenization for nonlinear conduction in
449 heterogeneous materials using model reduction. *Comp. Mater. Sci.*, 42, 704-712,
450 <https://doi.org/10.1016/j.commatsci.2007.11.001>, 2008.

451 Motulsky, H. J. and Ransnas, L. A.: Fitting curves to data using nonlinear regression: a practical and
452 nonmathematical review, *Faseb J.*, 1, 365-374. <https://doi.org/10.1096/fasebj.1.5.3315805>, 1987.

453 Pan, H., Guo, Z., Wang, Y., and Lv, X.: Application of the EMD method to river tides, *J. Atmos. Ocean. Tech.*,
454 35, 809-819, <https://doi.org/10.1175/JTECH-D-17-0185.1>, 2018.

455 Pearson, R. K. and Pottmann, M.: Gray-box identification of block-oriented nonlinear models, *J. Process*
456 *Contr.*, 10, 301-315, [https://doi.org/10.1016/S0959-1524\(99\)00055-4](https://doi.org/10.1016/S0959-1524(99)00055-4), 2000.

457 Reynolds, R. W., Smith, T. M., Liu, C., Chelton, D. B., Casey, K. S., and Schlax., M. G.: Daily high-
458 resolution-blended analyses for sea surface temperature, *J. Climate*, 20, 5473-5496,
459 <https://doi.org/10.1175/2007JCLI1824.1>, 2007.

460 Sadeghifar, T., Motlagh, M. N., Azad, M. T., and Mahdizadeh, M. M.: Coastal wave height prediction using
461 Recurrent Neural Networks (RNNs) in the south Caspian Sea, *Mar. Geod.*, 40, 454-465,
462 <https://doi.org/10.1080/01490419.2017.1359220>, 2017.

463 Savitha, R. and Mamun, A. A.: Regional ocean wave height prediction using sequential learning neural
464 networks, *Ocean Eng.*, 129: 605-612, <https://doi.org/10.1016/j.oceaneng.2016.10.033>, 2017.

465 Sukresno, B., Hanintyo, R., Kusuma, D. W., Jatisworo, D., and Murdimanto., A.: Three-way error analysis
466 of sea surface temperature (SST) between HIMAWARI-8, buoy, and mur SST in SAVU Sea, *Int. J.*
467 *Remote Sens. Earth Sci.*, 15, 25-36, <https://doi.org/10.30536/j.ijreses.2018.v15.a2855>, 2018,

468 Takakura, T., Kawamura, R., Kawano, T., Ichiyangi, K., Tanoue, M., and Yoshimura, K.: An estimation of
469 water origins in the vicinity of a tropical cyclone's center and associated dynamic processes, *Clim.*
470 *Dynam.*, 50, 555-569, <https://doi.org/10.1007/s00382-017-3626-9>, 2018.

- 471 Tang, L., Dai, W., Yu, L., and Wang, S.: A novel CEEMD-based EELM ensemble learning paradigm for crude
472 oil price forecasting, *Int. J. Inf. Tech. Decis.*, 14, 141-169, <https://doi.org/10.1142/S0219622015400015>,
473 2015.
- 474 Wang, S., Zhang, N., Wu, L., and Wang, Y.: Wind speed forecasting based on the hybrid ensemble empirical
475 mode decomposition and GA-BP neural network method, *Renew. Energ.*, 94, 629-636,
476 <https://doi.org/10.1016/j.renene.2016.03.103>, 2016.
- 477 Wang, W., Chau, K., Xu, D., and Chen, X.: Improving forecasting accuracy of annual runoff time series using
478 ARIMA based on EEMD decomposition, *Water Resour. Manag.*, 29, 2655-2675,
479 <https://doi.org/10.1007/s11269-015-0962-6>, 2015.
- 480 Wang, W., Tang, R., Li, C., Liu, P., and Luo, L.: A BP neural network model optimized by Mind Evolutionary
481 Algorithm for predicting the ocean wave heights, *Ocean Eng.*, 162, 98-107,
482 <https://doi.org/10.1016/j.oceaneng.2018.04.039>, 2018.
- 483 Wang, Y., Wilson, P. A., Zhang, M., and Liu, X.: Adaptive neural network-based backstepping fault tolerant
484 control for underwater vehicles with thruster fault, *Ocean Eng.*, 110, 15-24,
485 <https://doi.org/10.1016/j.oceaneng.2015.09.035>, 2015.
- 486 Wiedermann, M., Donges, J. F., Handorf, D., Kurths, J., and Donner, R. V.: Hierarchical structures in
487 Northern Hemispheric extratropical winter ocean–atmosphere interactions, *Int. J. Climatol.*, 37, 3821-
488 3836, <https://doi.org/10.1002/joc.4956>, 2017.
- 489 Wu, L. C., Kao, C. C., Hsu, T. W., Jao K. C. and Wang, Y. F.: Ensemble empirical mode decomposition on
490 storm surge separation from sea level data, *Coast. Eng. J.*, 53, 223-243,
491 <https://doi.org/10.1142/S0578563411002343>, 2011.
- 492 [Wu Z., Schneider E. K. and Kirtman B. P.: The modulated annual cycle: an alternative reference frame for](#)
493 [climate anomalies, *Clim. Dyna.*, 31\(7-8\): 823-841, <https://doi.org/10.1007/s00382-008-0437-z>, 2008.](#)
- 494 Wu, Z. and Huang, N. E.: Ensemble empirical mode decomposition: a noise-assisted data analysis method,
495 *Adv. Adap. Data Anal.*, 1, 1-41, <https://doi.org/10.1142/S1793536909000047>, 2009.
- 496 Wu Z., Jiang C., Chen J., Long Y., Deng B. and Liu X.: Three-Dimensional Temperature Field Change in the
497 South China Sea during Typhoon Kai-Tak (1213) Based on a Fully Coupled Atmosphere–Wave–Ocean
498 Model, *Water*, 11(1): 140, <https://doi.org/10.3390/w11010140>, 2019a.
- 499 Wu Z., Jiang C., Deng B., Chen J., Long Y., Qu K. and Liu X.: Numerical investigation of Typhoon Kai-tak
500 (1213) using a mesoscale coupled WRF-ROMS model, *Ocean Eng.*, 175: 1-15.

501 <https://doi.org/10.1016/j.oceaneng.2019.01.053>, 2019b.

502 Yeh, J. R., Shieh, J. S., and Huang, N. E.: Complementary ensemble empirical mode decomposition: A novel
503 noise enhanced data analysis method, *Adv. Adap. Data Anal.*, 2, 135-156,
504 <https://doi.org/10.1142/S1793536910000422>, 2010.

505 Zheng, X. T., Xie, S. P., Lv, L. H., and Zhou, Z. Q.: Intermodel uncertainty in ENSO amplitude change tied
506 to Pacific Ocean warming pattern, *J. Climate*, 29, 7265-7279, <https://doi.org/10.1175/JCLI-D-16-0039.1>,
507 2016.

508 Zhu, J., Huang, B., Kumar, A., and Kinter, J. L.: Seasonality in prediction skill and predictable pattern of
509 tropical Indian Ocean SST, *J. Climate*, 28, 7962-7984, <https://doi.org/10.1175/JCLI-D-15-0067.1>, 2015.

510